Research Square

Preprints are preliminary reports that have not undergone peer review.
They should not be considered conclusive, used to inform clinical practice,
or referenced by the media as validated information.

Attenuated Acute Microglial Responsiveness in Participants with Alzheimer's Disease: An In Vivo LPS Challenge [11C]PBR28 TSPO-PET Pilot Study

Arash Salardini

Salardini@uthscsa.edu

The University of Texas Health Science Center at San Antonio

Arsalan Hashemi-Aghdam

Dana-Farber Cancer Institute

Ryan S. O'Dell

Yale University

Ansel Hillmer

University of Michigan–Ann Arbor

Daniel F. Camacho

Yale University

Katie M. van Dyck

St. Lawrence University

Kimberly Nelsen

Yale University

Audrey Ruan

Yale University

Stephen M. Strittmatter

Yale University

Richard E. Carson

Yale University

Kelly P. Cosgrove

Yale University

Christopher H. van Dyck

Yale University

Adam P. Mecca

Yale University

Article

Keywords: Neuroinflammation, Microglia, TSPO-PET, Lipopolysaccharide, Alzheimer's disease, Immune challenge, APOE, Cytokines

Posted Date: March 4th, 2026

DOI: https://doi.org/10.21203/rs.3.rs-9012605/v1

License: This work is licensed under a Creative Commons Attribution 4.0 International License.
Read Full License

Additional Declarations: No competing interests reported.

Attenuated Acute Microglial Responsiveness in Participants with Alzheimer's Disease: An In Vivo LPS Challenge [^{11}C]PBR28 TSPO-PET Pilot Study

Arash Salardini, MD[1,2,3*], Arsalan Hashemi-Aghdam, MD[4], Ryan S. O'Dell, MD, PhD[5,6,7], Ansel T. Hillmer, PhD[8], Daniel F. Camacho, MD, PhD[7], Katie M. van Dyck[9], Kimberly C. Nelsen[5], Audrey Ruan[5], Stephen M. Strittmatter, MD, PhD[5], Richard E. Carson, PhD[5], Kelly P. Cosgrove, PhD[5], Christopher H. van Dyck, MD[5,6†], Adam P. Mecca, MD, PhD[5,6†]

[1]*Department of Neurology, UT Health Science Center, San Antonio, TX, USA*

[2]*Glenn Biggs Institute for Alzheimer's and Neurodegenerative Diseases, UT Health San Antonio, TX, USA*

[3]*South Texas Alzheimer's Disease Research Center, UT Health San Antonio, TX, USA*

[4]*Dana-Farber Cancer Institute, MA, USA*

[5]*Yale School of Medicine, New Haven, CT, USA*

[6]*Alzheimer's Disease Research Unit, Department of Psychiatry, Yale School of Medicine, New Haven, CT, USA*

[7]*Department of Psychiatry, Yale School of Medicine, New Haven, CT, USA*

[8]*Department of Radiology, University of Michigan, Ann Arbor, MI, USA*

[9]*St. Lawrence University, Canton, NY, USA*

†Authors contributed equally

***Corresponding author:** Arash Salardini, MD. Center for Brain Health, Glenn Biggs Institute for Alzheimer's and Neurodegenerative Disease, Department of Neurology, UT Health San Antonio, 4940 Charles Katz Dr., San Antonio, TX 78229. Email: salardini@uthscsa.edu

Abstract

Background: Elevated TSPO-PET binding in Alzheimer's disease (AD) is widely interpreted as increased microglial activity, yet whether these cells retain functional capacity for responses protective against amyloid and other pathologies remains unknown. We conducted a proof-of-concept study using in vivo lipopolysaccharide (LPS) challenge to assess dynamic microglial responsiveness.

Methods: Eleven participants (5 amyloid-negative controls, 6 amyloid-positive clinical AD) underwent serial [^{11}C]PBR28 TSPO-PET before and 3 hours after low-dose intravenous LPS (0.4 ng/kg). The prespecified primary outcome was parietal cortex microglial activity response index (MARI = [$V_{T,post}$ – $V_{T,pre}$]/$V_{T,pre}$). Secondary outcomes included MARI across 10 additional brain regions (FDR-corrected) and peripheral cytokines (n = 7). Given limited sample size, we prioritized effect size estimation with bootstrap 95% confidence intervals.

Results: Participants with clinical AD demonstrated markedly reduced microglial activity (parietal MARI: 0.18 ± 0.13 vs 0.36 ± 0.14; Cohen's d = 1.29, bootstrap 95% CI: 0.15–2.43). The responder rate (MARI > 0.20) was 100% in controls versus 33% in AD (Fisher's p = 0.061). The magnitude of blunted responses appeared consistent across brain regions (median effect size r = 0.53; 6/11 regions survived FDR q < 0.10). Peripheral cytokine responses paralleled central findings, with IL-6 MARI correlating with parietal brain MARI (ρ = 0.70) in the paired subset (n = 5).

Conclusions: This study provides preliminary in vivo evidence that AD is characterized by attenuated rather than intensified acute neuroinflammatory responses. The convergence of central and peripheral immune blunting suggests systemic dysfunction. These hypothesis-generating findings warrant replication in larger, age-matched cohorts.

Keywords: Neuroinflammation, Microglia, TSPO-PET, Lipopolysaccharide, Alzheimer's disease, Immune challenge, APOE, Cytokines

Background

Neuroinflammation plays a key role in Alzheimer's disease (AD), as genetic and molecular factors connect immune pathways to its incidence risk and progression [1,2]. In vivo imaging of the 18-kDa translocator protein (TSPO) has enabled quantification of activated microglia, with cross-sectional studies consistently reporting elevated binding in AD [3,4]. However, static TSPO measurements cannot differentiate between beneficial, adaptive activity (in response to diseases associated molecular patterns) and harmful chronic inflammation linked to impaired immune function.

Single-cell and single-nucleus transcriptomic analyses have identified distinct microglial phenotypes in AD brain tissue, characterized by altered homeostatic and inflammatory gene expression [5–8]. The functional capacity of these phenotypes, shaped by time, environment, genetics, age, and past exposures, remains poorly understood. Notably, human microglial transcriptomic signatures show limited overlap with murine disease-associated microglia (DAM) profiles [9,10], underscoring the need for functional characterization of microglial states in human disease. Immune challenge paradigms offer a complementary approach: low-dose intravenous lipopolysaccharide (LPS) activates Toll-like receptor 4 (TLR4) signaling, producing robust, measurable increases in brain TSPO binding within hours in healthy individuals [11, 12, 13].

We propose three possible functional phenotypes of microglia in AD associated with three different outcomes in this study (Figure 1A). If AD is characterized by a simple excess of microglial activity, then patients should have heightened microglial activity at baseline and stronger responses to LPS stimulation. Conversely, if persistent exposure to amyloid and tau pathology leads to microglial fatigue, then patients should exhibit lower baseline activity and weaker responses to LPS. Finally, if microglia generate excessive but dysfunctional neuroinflammation that is disconnected from environmental signals and not protective against amyloid toxicity, then patients should show higher baseline activity but lower LPS reactivity. This study thus introduces a dynamic functional phenotyping

approach to directly test microglial responsiveness in AD.

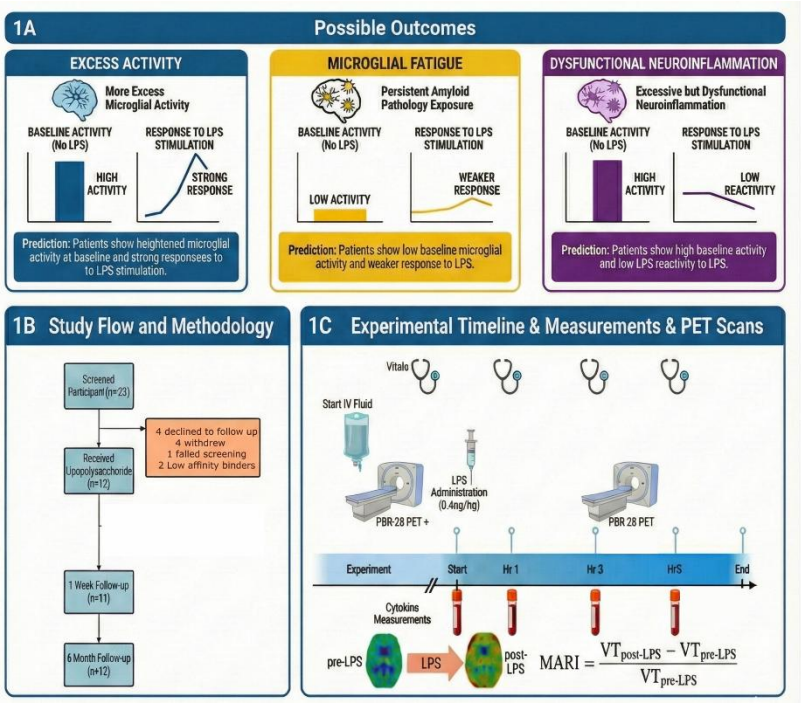


Figure 1. Study design and MARI concept. (A) The three possible functional phenotypes of microglia and the predicted outcome in this experiment. (B) CONSORT flow diagram. Of 23 screened participants, 12 received LPS and completed the study. (C) Study timeline: baseline PET, LPS administration (0.4 ng/kg IV), post-LPS PET at 3 hours; cytokine measurements at 0, 1, 3, 5 hours in subset (n = 7).

Methods

Study design and participants

This single-site prospective pilot study (NCT04057807) was approved by the Yale University Institutional Review Board. Between 2018–2020, 23 participants were screened, and 12 individuals were enrolled and received LPS; 12 completed the study and 11 had analyzable PET scans and one was excluded as technical failure of scan (Figure 1B). The final cohort comprised 5 amyloid-negative cognitively normal controls (3 Female/ 2 Male; mean age 69.6 ± 8.4 years; Clinical Dementia Rating global score [CDR] = 0, Mini Mental Status Exam [MMSE] > 26) and 6 amyloid-positive participants with AD (5 Female / 1 Male; mean age 75.2 ± 2.2 years; 2 dementia, 4 Mild Cognitive Impairment, MCI) diagnosed per NIA-AA criteria [14], with CDR 0.5–1.0 and Montreal Cognitive Assessment (MoCA) ≥ 17. Key exclusions included significant neurological disease other than AD, active infection, autoimmune conditions, immune-modulating medications within 3 weeks, and low-affinity binding status for the rs6971 TSPO polymorphism [15]. All participants provided written informed consent.

LPS administration and safety monitoring

Clinical Center Reference Endotoxin (CCRE; *E. coli* O:113:H10:K-negative; NIH) was administered as a single IV bolus at 0.4 ng/kg following an 8-hour fast. This dose produces reliable systemic and central immune activation while maintaining an acceptable safety profile in older adults [11-13]. Vital signs were monitored every 15 minutes for 6 hours. Delirium screening (Confusion Assessment Method) was performed at 48 hours; functional assessment (ADCS-ADL) and cognitive testing at 1 week; and comprehensive neuropsychological follow-up at 6 months.

PET imaging acquisition

[^{11}C]PBR28 PET scans (120 min dynamic acquisition) were performed pre-LPS and approximately 3 hours post-LPS on a High-Resolution Research Tomograph (HRRT; Siemens) (Figure 1C). Mean injected activity was 540 ± 193 MBq with molar activity of 215 ± 148 MBq/nmol and injected mass of 1.6 ± 1.8 μg (Additional File 1). Images were reconstructed using the Motion-compensation OSEM List-mode Algorithm for Resolution-recovery (MOLAR) with event-by-event motion correction via Vicra tracking.

For nine participants, both scans were completed on the same day (5–6-hour interval). For three participants, tolerability considerations required scheduling scans on separate days (intervals of 77–175 hours); no changes in medical status occurred during these intervals. The critical 3-hour interval between LPS administration and post-LPS scan acquisition was maintained for all participants.

Arterial blood sampling was performed throughout scanning for metabolite-corrected input functions. Plasma free fraction (f_P) was measured by ultrafiltration in triplicate. Mean f_P was 0.018 ± 0.005, with no significant difference between controls (0.015 ± 0.004) and AD (0.020 ± 0.004; $p = 0.12$).

Image analysis

Structural magnetic resonance imaging (MRI) was acquired on a 3T Siemens Trio using MPRAGE. A summed motion corrected PET image was used to create a registration between the MRI and PET scans for each participant using a mutual information algorithm with six degrees of freedom (FLIRT,

FSL 3.2; Analysis Group; FMRIB, Oxford, UK). The native MRI was then co-registered to the Montreal Neurological Institute (MNI) template space with a nonlinear transformation algorithm (BioImage Suite; http://www.bioimagesuite.com) for Region of Interest (ROI) definition. Distribution volumes (V_T) were estimated using multilinear analysis-1 (MA1) with t* = 30 min [16]. Partial volume correction was not applied given the within-subject nature of the design.

Outcome measures

- Primary outcome (prespecified): Parietal cortex MARI = $(V_{T,post} - V_{T,pre})/V_{T,pre}$. The parietal lobe was chosen as an area with significant increases in [11C]PBR binding due to AD [3].
- Secondary outcomes: (1) MARI in 10 additional regions (FDR-corrected); (2) responder analysis (MARI > 0.20, based on published test-retest variability [17]; (3) peripheral cytokine reaction (fold-change from baseline).
- Exploratory analyses: Age adjustment, APOE ε4 stratification, regional pattern analysis.

Peripheral cytokines

In 7 participants (4 controls, 3 AD), blood samples were collected at baseline and 1, 3, and 5 hours post-LPS. Cytokines were measured using a 65-plex Luminex panel (Bio-Rad Bio-Plex 200). Five participants had paired PET and cytokine data.

Statistical analysis

Given pilot sample size (n = 11), we employed an estimation statistics framework [18]: Cohen's d with Hedges' correction and bootstrap 95% CIs (10,000 resamples, BCa method); rank-biserial correlation (r) as nonparametric effect size. Responder analysis used Fisher's exact test. Regional analyses applied Benjamini-Hochberg FDR correction ($q < 0.10$). Leave-one-out sensitivity analyses assessed robustness. Analyses used Python 3.9 (scipy, statsmodels).

Results

Safety and baseline characteristics

LPS was well tolerated with expected transient flu-like symptoms (Table 1). No participants experienced a true fever (using a threshold of temperature greater than 100.4°F) during the course of the study. Three participants experienced low grade fever (defined as temperature between 99.1 and 100.4°F) at any time during vitals monitoring. One of these participants also complained of fatigue, chills, and bilateral shoulder ache which preceded the low-grade fever and lasted less than one hour, and another of these participants complained of mild headache and feeling chilly. Two patients complained of allergic or cold symptoms including eye or sinus discomfort or congestion. One participant experienced prolonged bleeding after arterial line removal, requiring 75 minutes of pressure to the site prior to resolution. Groups were similar in education (16.7 vs 16.5 years) and sex distribution but differed in age (AD: 75.2 ± 2.2 vs controls: 69.6 ± 8.4 years; d = 0.91) and cognitive function (MoCA: 21.5 vs 26.8; d = 1.70) (Table 2). Baseline parietal V_T did not differ significantly (AD: 5.12 ± 1.29 vs controls: 4.59 ± 1.35; d = 0.40; p = 0.66).

Table 1. Adverse events following LPS administration (CTCAE v5.0)

Adverse Event	Total Cohort (n=12)	Grade
Low-grade fever (99.1–100.4°F)	3 (25%)	1
Chills	2 (17%)	1
Fatigue	1 (8%)	1
Headache	1 (8%)	1
Myalgia (shoulder)	1 (8%)	1
Upper respiratory/allergic symptoms	2 (17%)	1
Prolonged bleeding at arterial line site	1 (8%)	1
True fever (>100.4°F)	0	—
Delirium (CAM+)	0	—
Serious adverse events	0	—

All events were transient and self-limiting. Low-grade fever defined as 99.1–100.4°F. The prolonged bleeding event required 75 minutes of manual pressure but resolved without further intervention. CAM = Confusion Assessment Method.

Table 2. Participant characteristics for image analysis sample

Characteristic	Controls (n=5)	AD (n=6)	d [95% CI]	p
Age, years	69.6 ± 8.4	75.2 ± 2.2	0.91 [−0.42, 2.24]	0.09
Sex, M/F	3/2	5/1	—	0.55
Education, years	16.5 ± 2.8	16.7 ± 1.6	0.09 [−1.18, 1.36]	0.93
MoCA	26.8 ± 2.4	21.5 ± 3.7	1.70 [0.32, 3.08]	0.02
CDR-SB	0	3.0 ± 1.8	—	<0.01
APOE ε4+, n (%)	2 (40%)	4 (67%)	—	0.57
TSPO HAB, n (%)	3 (60%)	5 (83%)	—	0.55
Amyloid PET positive	0 (0%)	6 (100%)	—	<0.01
Parietal V_T (baseline)	4.59 ± 1.35	5.12 ± 1.29	0.40 [−0.89, 1.69]	0.66

Values are mean ± SD or n (%). HAB = high-affinity binder. CDR-SB = Clinical Dementia Rating Sum of Boxes.

Primary outcome: Attenuated MARI in AD

AD participants showed markedly attenuated microglial activity (Figure 2). Parietal MARI was 0.18 ± 0.13 versus 0.36 ± 0.14 in controls—a large effect: Cohen's d = 1.29 (bootstrap 95% CI: 0.15–2.43); rank-biserial r = 0.60. Critically, 100% of controls (5/5) were responders (MARI > 0.20) compared to only 33% of AD (2/6) (Fisher's p = 0.061), suggesting group differences extend beyond mean response magnitude. Leave-one-out analysis yielded stable effect sizes (d range: 1.03–1.59).

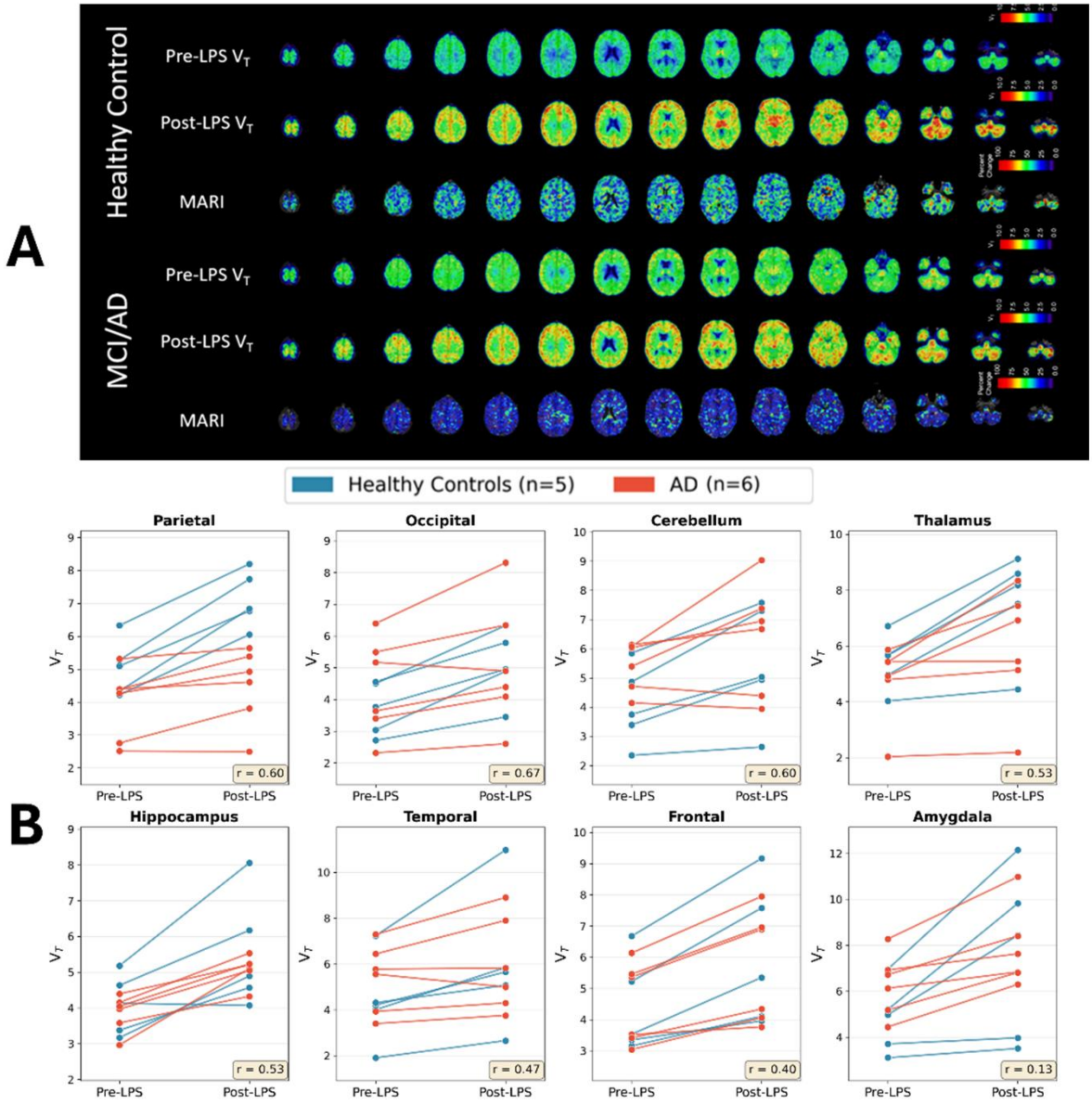


Figure 2. Primary outcome and regional analysis. (A) Representative parametric MARI, post-LPS V_T, and pre-LPS V_T images for all AD (left) and Healthy Control (right) participants, demonstrating visually apparent attenuation of LPS-induced TSPO binding increases in AD. (B) Regional comparison of pre-LPS V_T, post-LPS V_T, and MARI across brain regions by diagnostic group.

Secondary outcomes: Regional consistency

Blunted responses were consistent across all 11 brain regions (Table 3, Figure 3). Median effect size was r = 0.53. Six regions survived FDR correction at $q < 0.10$, occipital ($r = 0.67$, $p_{FDR} = 0.082$), cerebellum, parietal, caudate, thalamus, and hippocampus. This anatomical consistency reinforces

confidence in the primary finding. Exploratory three-group analysis (HC vs MCI vs dementia) suggested a gradient of attenuation, with MCI showing intermediate MARI values (0.22–0.32) between controls (0.31–0.46) and dementia (0.05–0.14) (Additional File 5).

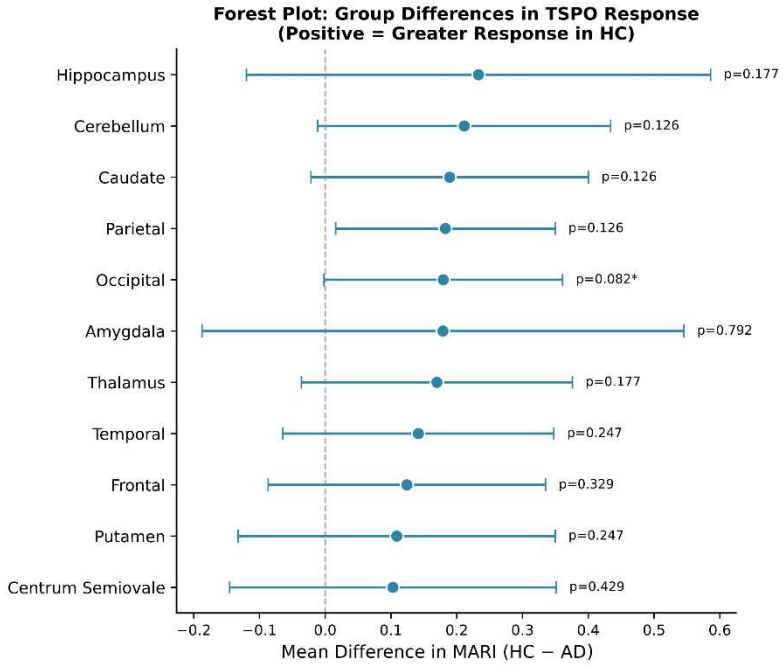


Figure 3. Regional effect sizes. Forest plot of rank-biserial correlation (r) with 95% bootstrap confidence intervals for all 11 brain regions. Dashed vertical line indicates r = 0 (no effect). Asterisks denote regions significant at FDR q < 0.10.

Table 3. Regional brain MARI values

Region	Controls	AD	r	p	p_{FDR}	Sig
Occipital	0.35 ± 0.14	0.17 ± 0.17	0.67	0.082	0.082	*
Parietal†	0.36 ± 0.14	0.18 ± 0.13	0.60	0.126	0.095	*
Cerebellum	0.40 ± 0.16	0.19 ± 0.22	0.60	0.126	0.095	*
Caudate	0.36 ± 0.19	0.16 ± 0.20	0.60	0.126	0.095	*
Thalamus	0.36 ± 0.10	0.19 ± 0.23	0.53	0.177	0.098	*
Hippocampus	0.46 ± 0.32	0.23 ± 0.26	0.53	0.177	0.098	*

*†Primary endpoint (prespecified). *Significant at FDR q < 0.10. r = rank-biserial correlation. Full 11-region table in Additional File 3.*

Peripheral cytokine responses

Microglial Activity Response Index (MARI) was calculated as the fold-change from baseline to 3 hours post-LPS [(Concentration$_{3h}$ − Concentration$_{0h}$) / Concentration$_{0h}$]. Consistent with the blunted central TSPO-PET response, AD participants demonstrated markedly attenuated peripheral cytokine responses compared to healthy controls. Six cytokines showed nominally significant group differences (all p = 0.057, Mann-Whitney U; Figure 4), with healthy controls exhibiting dramatically higher MARI values for IL-1RA (HC: 397.7 vs AD: 0.37), G-CSF (54.0 vs 1.1), IL-6 (50.7 vs 1.9), MIP-1α (28.1 vs 0.35), MCP-2 (5.4 vs 0.003), and IL-16 (0.74 vs −0.12). Time-course analysis revealed that healthy controls mounted robust cytokine responses peaking at 3 hours post-LPS—with mean IL-6 rising from 0.5 to 24 pg/mL and IL-1RA surging to approximately 1000 pg/mL—while AD participants showed flat or minimal responses throughout the 5-hour observation period. Although these findings did not survive FDR correction given the small sample size (n=4 HC, n=3 AD), the effect sizes were maximal (r = 1.0) for all top cytokines, indicating complete group separation and suggesting that the diminished innate immune responsiveness observed centrally via TSPO-PET extends to peripheral circulating immune cells.

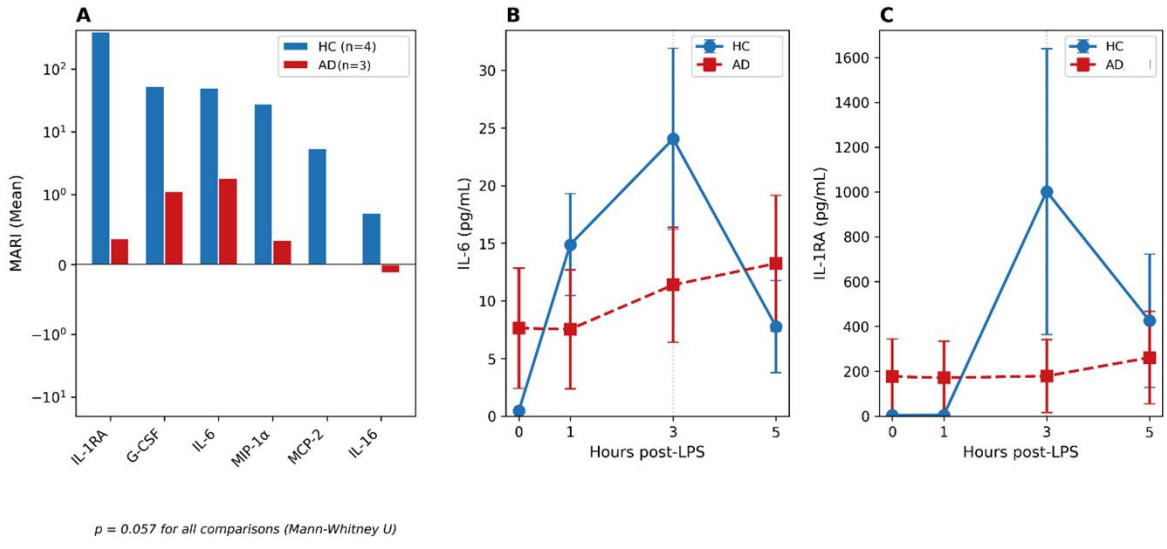


Figure 4. Serum cytokine responses to LPS challenge. (A) Mean cytokine reaction (fold-change from baseline to 3 hours post-LPS) for top differentially responding cytokines; all p = 0.057, Mann-Whitney U. (B–C) Time course of IL-6 and IL-1RA concentrations showing robust responses in HC with

attenuated responses in AD. Dotted lines indicate 3-hour timepoint. Data: mean ± SEM; HC n=4, AD n=3.

Exploratory analyses

Age. In an ANCOVA controlling for age, the diagnosis effect on parietal MARI remained in the same direction but was attenuated by ~34%, consistent with immunosenescence contributions.

APOE ε4 (hypothesis-generating). Unexpectedly, ε4 carriers showed higher MARI overall (0.32 ± 0.08 vs 0.20 ± 0.16; d = 0.91), while ε4-negative participants with AD (n = 2) showed near-zero responses (MARI = 0.03 ± 0.03). This contrasts with in vitro studies suggesting APOE4 microglia exhibits blunted LPS responsiveness due to a primed baseline state [19]. However, with only 2 ε4-negative AD patients, this finding is statistically fragile and must be interpreted as hypothesis-generating only.

Clinical correlations. In the AD group, higher parietal MARI was associated with lower CDR-SB (R^2 = 0.33, p = 0.065) and tended toward association with higher MoCA scores (R^2 = 0.21, p = 0.15), suggesting microglial responsiveness relates to clinical severity (Figure 5).

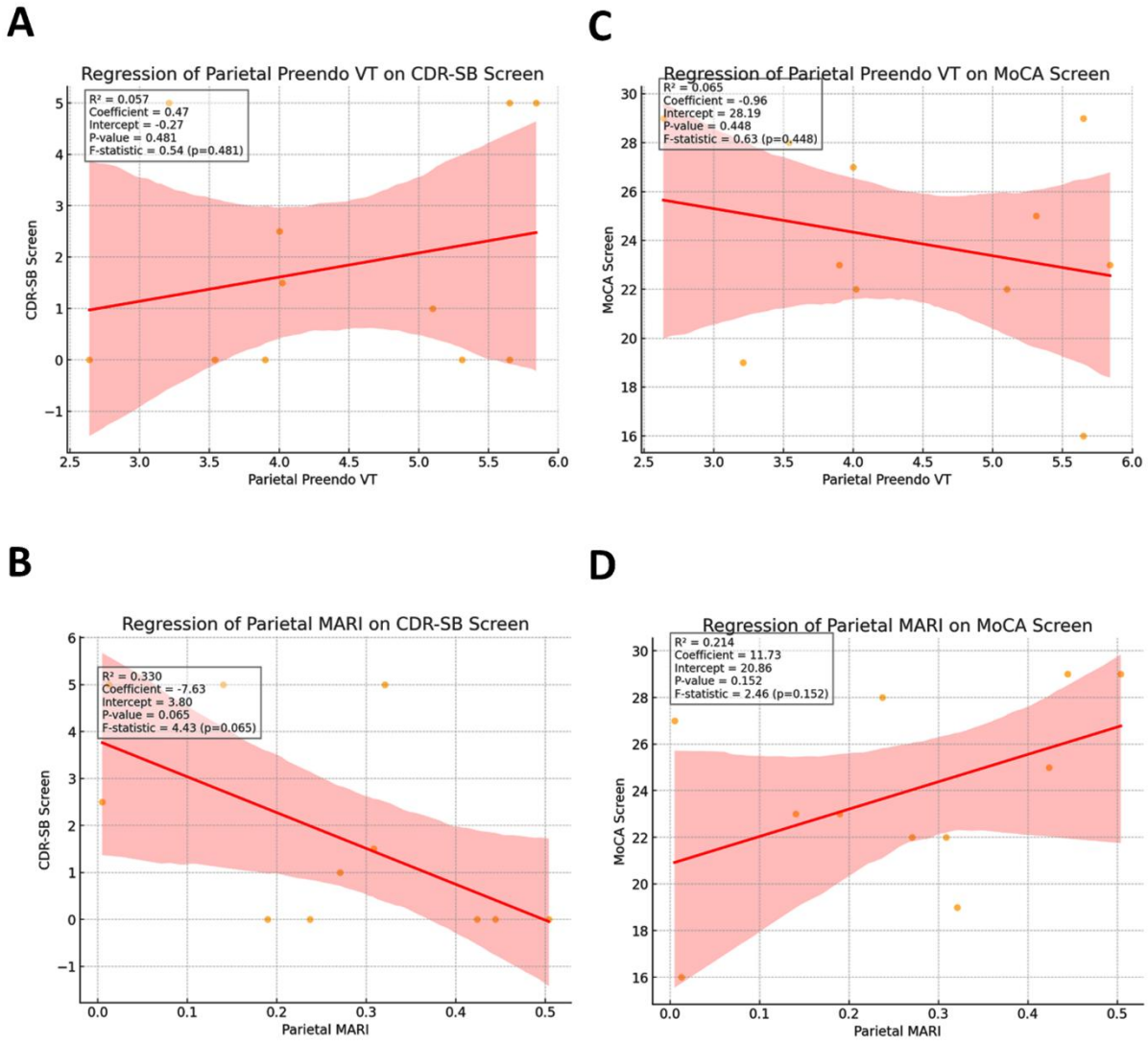


Figure 5. Clinical correlations. Relationships between parietal MARI and clinical outcomes. (A) Baseline V_T vs CDR-SB. (B) MARI vs CDR-SB (R^2 = 0.33, p = 0.065). (C) Baseline V_T vs MoCA. (D) MARI vs MoCA (R^2 = 0.21, p = 0.15). Higher MARI tends to associate with better clinical status.

Discussion

These findings offer preliminary in vivo evidence that acute neuroinflammatory responses to immune challenge may be attenuated rather than intensified in individuals with AD. Despite well-documented elevations in baseline TSPO binding [3,4], our data support that participants with AD may have a reduced capacity to mount additional responses when challenged with LPS. Five key findings emerge.

Safety:

The administration of LPS to older adults with healthy cognition and with AD was safe with only mild adverse events and no cognitive side effects. This finding is notable when compared to prior work [13], which utilized a higher dose of LPS and observed transient cognitive and behavioral shifts in the midst of peak systemic responses. Our data, utilizing a lower dose (0.4 ng/kg), demonstrate that this paradigm can be safely applied to AD populations without inducing delirium, functional decline, or cognitive decline.

Functional dysfunction rather than hyperactivity:

The large effect size (d = 1.29) and categorical responder difference (100% vs 33%) indicate this is not merely a quantitative reduction but a qualitative loss of inflammatory capacity in most AD participants. The pattern we observe—preserved baseline TSPO binding coupled with diminished acute responsiveness—has functional parallels to several described immune phenotypes, including T cell exhaustion from chronic antigen exposure [20], the senescence-associated secretory phenotype (SASP), and transcriptionally-defined microglial states in AD [5–8]. However, whether these in vivo imaging findings reflect a single mechanism or convergent dysfunction from multiple pathways cannot be determined from the present data.

A regional pattern consistent with progressive exhaustion:

Intriguingly, the regional pattern of effect sizes was inversely related to Braak tau staging (Figure S1-B): regions affected earliest by tau pathology (hippocampus, amygdala) showed the smallest group differences in MARI, while later-affected regions (thalamus, neocortex) showed the largest effects (d = 2.0–3.0 for thalamus, putamen, frontal cortex vs d = 0.8–1.4 for hippocampus, amygdala). This pattern could be consistent with progressive microglial exhaustion, wherein regions with longest exposure to pathology have already reached a functional floor, leaving less room to detect differential blunting of response. Alternatively, early affected regions may have experienced greater tissue loss or microglial depletion, reducing signal detectability.

Systemic immune dysfunction:

The parallel blunting of peripheral cytokine responses (IL-6, MCP-2, MIP-1α) and correlation between central and peripheral measures points to immune dysregulation extending beyond the CNS. Prior ex vivo studies found that LPS-stimulated cytokine release from peripheral blood cells decreases with AD severity [21,22], consistent with our in vivo findings. This systemic pattern suggests that microglial dysfunction may be one manifestation of broader immune senescence or exhaustion in AD.

Potential therapeutic implications.

If confirmed, these findings have implications for immunomodulatory therapeutic strategies. The failure of anti-inflammatory approaches such as NSAIDs in AD trials [23] may reflect a fundamental misconception: further suppressing an already weakened system provides no benefit. Instead, strategies aimed at restoring appropriate immune responsiveness, such as TREM2 agonism to enhance microglial phagocytic function [24] might better align with this pathophysiology. However, we emphasize these therapeutic considerations remain speculative pending replication.

Strengths and limitations

Key strengths include the novel application of an immune challenge paradigm to AD, rigorous PET methodology (arterial input functions, binding affinity genotyping, event-by-event motion correction), and transparent statistical approach emphasizing effect size estimation. The consistency across 11 brain regions, concordance with peripheral cytokines, and biologically plausible regional pattern strengthen the results.

A number of limitations should be acknowledged. The sample size (n = 11 PET; n = 7 cytokines) yields wide confidence intervals (0.15–2.43). The AD group was numerically older, and while a sensitivity analysis with age-adjustment was performed, residual confounding cannot be excluded. The single 3-hour post-LPS PET timepoint may not have captured peak responses in all individuals. However, our serum cytokine and previous studies using this method support 3-hours post-LPS as the optimal timepoint. Finally, TSPO is expressed on multiple cell types beyond microglia, including astrocytes and endothelial cells, a well-known limitation of the technique.

Conclusions

This pilot study demonstrates the feasibility of LPS challenge with serial TSPO-PET in AD and provides preliminary evidence of attenuated acute neuroinflammatory capacity. Effect sizes were large but imprecisely estimated. The inverse relationship between regional effect sizes and Braak staging suggests progressive exhaustion with disease duration. These hypothesis-generating findings warrant replication in larger, age-matched cohorts with serial post-LPS imaging before informing therapeutic development. If validated, this dynamic functional phenotyping approach could serve as a biomarker of microglial competence for stratifying patients and monitoring immunomodulatory interventions.

Declarations

Ethical Approval and Consent to participate: This study was approved by the Yale University Institutional Review Board (HIC number 1611018611). Written informed consent was obtained from all participants or their legally authorized representatives.

Consent for publication: Not applicable.

Availability of data and materials: De-identified participant-level data and analysis code are available upon reasonable request.

Competing interests: None declared.

Funding: This project was funded by 1R21AG054213-01 (PI- Salardini).

Authors' contributions: AS: conceptualization, analysis, writing. project PI. AHA: data curation, analysis. RSO: data curation, investigation. ATH: methodology, image analysis, investigation. DFC: investigation. KMVD: investigation. KN, AR, JL: data collection. REC: methodology, resources. SMS: resources, supervision. KC: methodology, resources. CHvD: conceptualization, supervision, funding. APM: supervision, analysis, PI after 2020. All authors reviewed and approved the final manuscript.

Acknowledgements: Not applicable.

Supplementary files

Additional file S1. PET acquisition parameters. Per-scan injected activity, specific activity, mass dose, f_P, scan timing.

Additional file S2. De-identified participant data. Demographics, genotypes, regional V_T and MARI values.

Additional file S3. Full regional analysis (11 regions) with effect sizes and leave-one-out sensitivity.

Additional file S4. Cytokine data with subject mapping to PET.

Additional file S5. Supplementary figures: (a) Three-group analysis (HC vs MCI vs dementia) showing gradient of MARI attenuation; (b) Regional effect sizes showing inverse relationship with Braak staging; (c) V_T changes across ROIs; (d) Baseline V_T vs MARI relationships; (e) APOE ε4 exploratory analysis.

References

1. Heneka MT, Carson MJ, El Khoury J, et al. Neuroinflammation in Alzheimer's disease. Lancet Neurol. 2015;14(4):388–405.
2. Bellenguez C, Küçükali F, Jansen IE, et al. New insights into the genetic etiology of Alzheimer's disease and related dementias. Nat Genet. 2022;54(4):412–36.
3. Kreisl WC, Lyoo CH, McGwier M, et al. In vivo radioligand binding to translocator protein correlates with severity of Alzheimer's disease. Brain. 2013;136(Pt 7):2228–38.
4. Edison P, Archer HA, Gerhard A, et al. Microglia, amyloid, and cognition in Alzheimer's disease. Neurobiol Aging. 2008;29(3):412–9.
5. Mathys H, Davila-Velderrain J, Peng Z, et al. Single-cell transcriptomic analysis of Alzheimer's disease. Nature. 2019;570(7761):332–7.
6. Olah M, Menon V, Habib N, et al. Single cell RNA sequencing of human microglia uncovers a subset associated with Alzheimer's disease. Nat Commun. 2020;11:6129.

7. Sun N, Victor MB, Park YP, et al. Human microglial state dynamics in Alzheimer's disease progression. Cell. 2023;186(20):4386–4403.
8. Gerrits E, Brouwer N, Kooistra SM, et al. Distinct amyloid-β and tau-associated microglia profiles in Alzheimer's disease. Acta Neuropathol. 2021;141(5):681–696.
9. Keren-Shaul H, Spinrad A, Weiner A, et al. A unique microglia type associated with restricting development of Alzheimer's disease. Cell. 2017;169(7):1276–90.
10. Sala Frigerio C, Bhattacharya A. Microglia in Alzheimer's disease at single-cell level: Are there common patterns in humans and mice? J Exp Med. 2021;218(9):e20202717.
11. Sandiego CM, Gallezot JD, Pittman B, et al. Imaging robust microglial activation after lipopolysaccharide administration in humans with PET. Proc Natl Acad Sci USA. 2015;112(40):12468–73.
12. Hannestad J, Subramanyam K, Dellagioia N, Planeta-Wilson B, Weinzimmer D, Pittman B, Carson RE. Glucose metabolism in the insula and cingulate is affected by systemic inflammation in humans. J Nucl Med. 2012 Apr;53(4):601-7.
13. Bonomi R, Hillmer AT, Woodcock E, Bhatt S, Rusowicz A, Angarita GA, Carson RE, Davis MT, Esterlis I, Nabulsi N, Huang Y, Krystal JH, Pietrzak RH, Cosgrove KP. Microglia-mediated neuroimmune suppression in PTSD is associated with anhedonia. Proc Natl Acad Sci U S A. 2024 Aug 27;121(35):e2406005121.
14. Jack CR Jr, Bennett DA, Blennow K, et al. NIA-AA Research Framework. Alzheimers Dement. 2018;14(4):535–62.
15. Owen DR, Yeo AJ, Gunn RN, et al. An 18-kDa translocator protein (TSPO) polymorphism explains differences in binding affinity. J Cereb Blood Flow Metab. 2012;32(1):1–5.
16. Ichise M, Toyama H, Innis RB, Carson RE. Strategies to improve neuroreceptor parameter estimation. J Cereb Blood Flow Metab. 2002;22(10):1271–81.
17. Park E, Gallezot JD, Delgadillo A, Liu S, Planeta B, Lin SF, O'Connor KC, Lim K, Lee JY, Chastre A, Chen MK, Seneca N, Leppert D, Huang Y, Carson RE, Bhagwagar Z, Pelletier D. (11)C-PBR28

imaging in multiple sclerosis patients and healthy controls: test-retest reproducibility and focal visualization of active white matter areas. Eur J Nucl Med Mol Imaging. 2015 Jun;42(7):1081-92.

18. Cumming G. The new statistics: why and how. Psychol Sci. 2014;25(1):7–29.
19. Friday CM, Stephens IO, Smith CT, Lee S, Satish D, Devanney NA, Cohen S, Morganti JM, Gordon SM, Johnson LA. APOE4 reshapes the lipid droplet proteome and modulates microglial inflammatory responses. Neurobiol Dis. 2025 Aug;212:106983.
20. Wherry EJ, Kurachi M. Molecular and cellular insights into T cell exhaustion. Nat Rev Immunol. 2015;15(8):486–99.
21. Magaki S, Mueller C, Bhattacharya A. Peripheral cytokine release in Alzheimer patients: correlation with disease severity. Neurobiol Aging. 2007;28(12):1904–16.
22. Munawara U, Catanzaro M, Xu W, et al. Hyperactivation of monocytes and macrophages in MCI patients contributes to the progression of Alzheimer's disease. Immun Ageing. 2021;18:29.
23. Heneka MT, Kummer MP, Weggen S, et al. NLRP3 is activated in Alzheimer's disease and contributes to pathology in APP/PS1 mice. Nature. 2013;493(7434):674–8.
24. Schlepckow K, Monroe KM, Kleinberger G, et al. Enhancing protective microglial activities with a dual function TREM2 antibody. EMBO Mol Med. 2020;12(4):e11227.

Supplementary Files

This is a list of supplementary files associated with this preprint. Click to download.

- AdditionalFile1PETParameters.csv
- AdditionalFile2ParticipantData.csv
- AdditionalFile3RegionalAnalysis.csv
- AdditionalFile4bCytokineSubjectLevel.csv
- AdditionalFile4aCytokineSummary.csv
- SupplementaryFigures.png